Finite Transducer Size Compensation in Two-Dimensional Photoacoustic Computed Tomography

Hakakzadeh, Soheil ; Mozaffarzadeh, Moein; Mostafavi, Seyed Masood; Amjadian, Mohammadreza ; Kavehvash, Zahra ; Verweij, Martin; de Jong, Nico

DOI
10.1109/IUS52206.2021.9593757

Publication date
2021

Document Version
Accepted author manuscript

Published in
2021 IEEE International Ultrasonics Symposium (IUS)

Finite Transducer Size Compensation in Two-Dimensional Photoacoustic Computed Tomography

Soheil Hakakzadeh[1], Moein Mozaffarzadeh[2], Seyed Masood Mostafavi[1], Mohammadreza Amjadian[1,3], Zahra Kavehvash[1,*], Martin Verweij[2,4] and Nico de Jong[2,4]

[1]*Department of Electrical Engineering, Sharif University of Technology, Tehran, Iran*
[2]*Department of Imaging Physics, Delft University of Technology, Delft, The Netherlands*
[3]*Department of Chemical and Biological Engineering, Hong Kong University of Science and Technology, Hong Kong SAR*
[4]*Department of Biomedical Engineering, Thoraxcenter, Erasmus Medical Center, Rotterdam, The Netherlands*

* *kavehvash@sharif.edu*

***Abstract*— In circular photoacoustic computed tomography, for data acquisition, a single-element transducer rotates around the region of interest (ROI). Due to the limited acceptance angle of the finite size transducer, the reconstructed image becomes blurred, and tangential resolution/contrast degrades in off-center locations in the ROI. In this paper, we propose a compensation method in which in addition to the circular scanning, the transducer rotates around its center (with specific angles) at each detection point. The superposition of these central rotations and non-rotated transducer mimics a virtual detector with a wide acceptance angle. The angles are calculated based on the central frequency and diameter of the transducer and the radius of the region-of-interest. Three types of numerical phantom (point-like, vasculature and Derenzo) were used to evaluate the performance of our method. Features of Olympus NDT, V326-SU transducer were used to assemble the numerical data. The results show that the proposed method provides better structural information by lowering the image blurring, improves the tangential resolution by 90% and increases peak signal-to-noise ratio by 14%.**

Keywords*— Photoacoustic imaging, Finite size transducer, virtual source. Resolution, Image blurring.

I. Introduction

Photoacoustic computed tomography (PACT) is a non-ionizing and safe imaging modality with many clinical applications [1]. In this imaging modality, a laser source irradiates the tissue of interest. Tissue chromophores absorber the optical energy and excite photoacoustic (PA) waves [2, 3]. PA waves are recorded by ultrasound transducers and finally used to reconstruct the optical absorption distribution of the tissue [4].

Two dimensional PACT can be used in three different arrangements: linear, circular limited-view and circular full-view. The quality of images obtained by the circular full-view arrangement is higher as it provides more angular views to record PA waves [5].

The most commonly used reconstruction technique is back-projection in which the transducer is assumed point-like [6]. A point-like transducer has a wide acceptance angle. If it is used in a circular full-view, the superposition of its field of view (FOV) from all the spatial sampling points fulfills the entire region of interest (ROI). This results in a location independent tangential resolution. In practice, however, this is not met since the acceptance angle of the finite size transducers limits the sideways view. This blurs the image and degrades the off-center resolution.

To tackle this issue, different methods have been developed over the past few years. Kalva and Pramanik [7] proposed a modified delay and sum algorithm (MDAS) in which each PA signal is back-projected from all the sub-elements defined on the transducer surface. Xiao, et al. [8] presented a combination of MDAS and sensitivity factor for further improvements. Wang, et al. [9] also proposed approximate back-projection in which a system matrix was used to compensate the time-delay and directivity pattern of a large aperture transducer. Positive and negative focused transducers or acoustic lenses can be used to mimic a virtual point detector with a wide acceptance angle [10, 11]. However, the sensitivity of these focused transducers/lenses is low. Moreover, deep learning, model-based and iterative reconstruction algorithms can also be helpful, but at the expense of a high computational cost [12].

In this paper, we present a method to compensation effects of the finite-size transducer in two-dimensional PACT. In our method, while a transducer rotates around the ROI, we additionally use central rotations (α) at each spatial sampling point (detection point). This is feasible with a conventional detection system by tilting the transducer and performing a new data acquisition for each central rotation.

II. Materials and Methods

In a 2D scenario, each point-absorber in the ROI generates a circular wave propagating in all the directions. Each direction of the PA wave represents a specific spatial frequency component along the tangential direction. With point-like detectors arranged in a full-view circular detection geometry, the maximum range of spatial frequency components are captured. This results in a location-independent tangential resolution.

The acceptance angle of a flat transducer is shown in Fig. 1(a). The -10 dB of its main lobe is calculated as follows:

$$\sin\theta_{MAX} = \frac{0.9\lambda}{D}, \tag{1}$$

where λ and D are the transducer wavelength corresponding to the low cut-off frequency and diameter,

respectively. The smaller the transducer diameter, the larger acceptance angle θ_{MAX} (wider FOV), for a constant wavelength. Due to the limited FOV of a finite size transducer, as the off-center distances increase, a lower range of spatial frequency components will be captured, resulting in a lower tangential resolution (i.e., extension of the point spread function (PSF) along the tangential direction). This extension is given by (2):

$$W(r) = \frac{rD}{R}, \tag{2}$$

where r is the distance from the center and R is the scanning radius.

Figure. 1(a) shows the schematic of the proposed method. At each scanning point, the transducer rotates centrally with α degrees to capture a wider range of spatial frequency components. The central rotation angles are calculated so that the edge of the beams in the rotated and non-rotated transducer overlap minimally. The central rotation angles can be given by:

$$\alpha_{c,n} = \sin^{-1}\frac{1.8n\lambda}{D}, \tag{3}$$

where, n is the number of required central rotations, which is from 1 to $N = \left\lfloor \frac{\left\lfloor \frac{R_{ROI}D}{0.9R\lambda} \right\rfloor - 1}{2} \right\rfloor$ and R_{ROI} is the radius of the ROI. It should be noted that the ROI must be located in the far field of the ultrasound transducer. In each scanning point, the superposition of the transducer and its central rotations can be considered as a virtual detector with an effective diameter D_v, which is given by (4).

$$D_v = \frac{0.9\lambda}{\sin(\sin^{-1}\frac{1.8\lambda N}{D} + \sin^{-1}\frac{0.9\lambda}{D})}. \tag{4}$$

This virtual detector captures the maximum range of spatial frequencies. The PSF extension along the tangential direction is given by:

$$W^v(r) = \frac{rD_v}{R}. \tag{5}$$

To reduce the number of scanning points in the proposed method, in each central rotation, the PA signal is only back-projected in the spatial range of its directivity pattern. The minimum number of required scanning points in the proposed method is given in (6):

$$N_v = \frac{K_c \cdot R_{ROI}}{\left\lfloor \frac{R_{ROI}D}{0.9R\lambda} \right\rfloor}, \tag{6}$$

where, K_c is wave-number corresponding to the high cut-off frequency of the transducer bandwidth.

III. Simultion Study and Results

A. Simulation study

K-wave [13] MATLAB toolbox was used to model the PA wave propagation. The imaging medium and grid size were 12 cm and 0.1 mm in both the directions, respectively. A transducer with a diameter of 6 mm, central frequency of 2.25 MHz, and bandwidth of 80% (features of Olympus NDT, V326-SU transducer) was used to assemble the data. The detection radius was 5.6 cm and divided into 450 scanning points for the conventional detection method. The 90 scanning points without a central rotation ($\alpha = 0$) and with central rotation (α) of -35º, -17º, 17º, 35º were used for implementing the proposed method. These central rotation angles and scanning points were calculated based on (3) and (6), respectively. Moreover, according to (4), the effective diameter (D_v) of the virtual detector is 1.2 mm. Two model was simulated: a) five-point target with a diameter of 0.3 mm to assess PSF extension along the tangential direction, and b) vasculature and Derenzo phantoms to evaluate the blurring effects, especially in regions close to the detection surface.

B. Results

Using the conventional detection geometry, as the off-center distances increases, the PSF extends along the tangential direction (Fig. 1(b)). This extension reaches 3.5 mm for 40 mm distances from the center (Fig. 1(b, d)). With the proposed method, the tangential resolution is almost constant in all the locations. The PSF extension in the proposed method reaches 0.5 mm for 40 mm off-center distance (Fig. 1(c, d)).

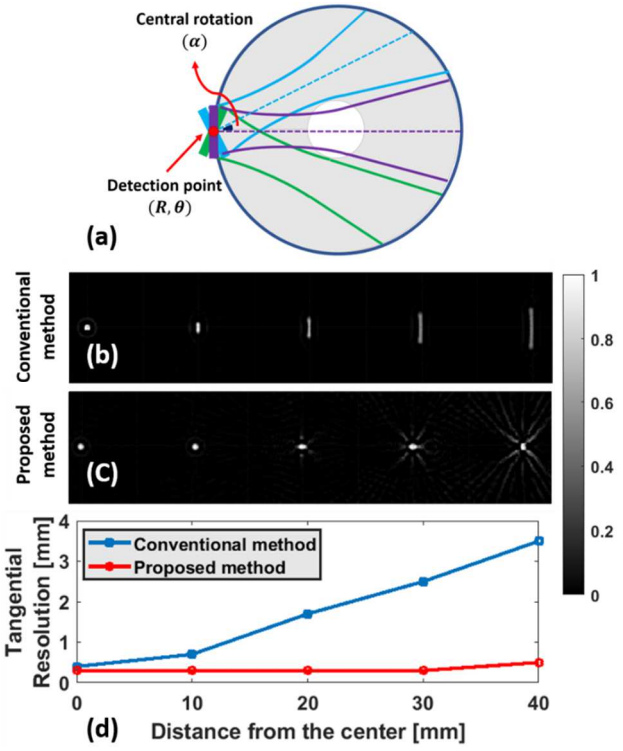

Fig. 1: (a) Schematic of the proposed detection approach. The reconstructed images with (b) the conventional and (c) the proposed method using point targets. (d) The tangential resolution for different off-center distances.

The extension of the PSF (due to conventional reconstruction) blurs the image, especially in close to the detection surface (Fig. 2(a)). The proposed method lowers down the blurring effect (see the blue-dashed circle in Fig. 2(d) and arrows in Fig. 2(b)), better distinguishes the targets (Fig. 2(g)), and increases the contrast ratio to 10.7 dB (measured 7.46 dB for the conventional approach). The PSNR of the yellow dashed line (see Fig. 2(c, d, g)) is

measured as 20.4 dB and 17.85 dB in the proposed and conventional methods, respectively, while the central PSF was not alter (Fig. 2(e, f)).

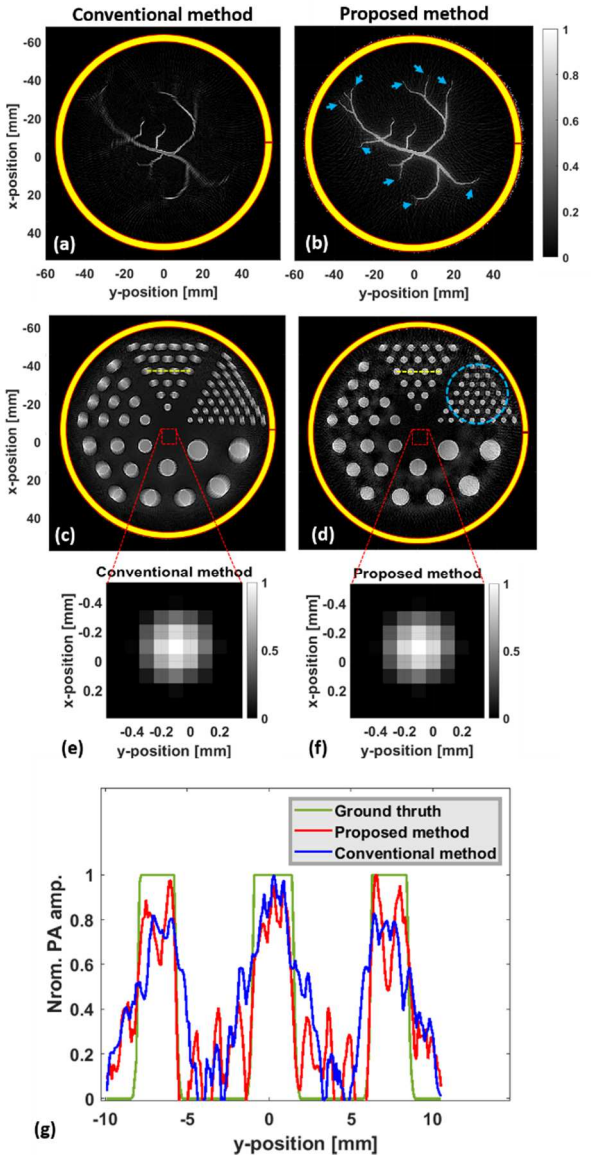

Fig. 2: (a, b) The reconstructed images with the conventional and proposed approach, respectively; the vasculature phantom was used. (c, d) The reconstructed images with the conventional and proposed approach, respectively; the Derenzo phantom was used. (e, f) The point spread function in the middle of ROI. (g) The 1D intensity profile indicated by the yellow dashed-line in (c, d).

IV. Discussion and Conclusion

In PACT, the acceptance angle of the transducer is limited due to the finite size of the transducer. Consequently, as the off-center distance increases, the captured range of spatial frequency components decreases, which degrades the tangential resolution. With our method. a location independent tangential resolution can be achieved as we synthesize a virtual point detector by rotating the transducer around its center. To reduce the number of scanning points and to avoid aliasing and other artifacts, the directivity pattern was contributed in back-projecting signals which led to a directional back-projection.

Our method has limitations. In practice, implementing central rotations based on the calculated angles may have a few errors (±1 degree), which induces artifacts to the reconstructed image. Moreover, applying these central rotations is time-consuming. Combining the proposed strategy with a ring array transducer could address this issue. However, the implementation of the proposed detection strategy would be different than rotating the element of the array. This would be a matter of our future studies.

References

[1] A. B. E. Attia *et al.*, "A review of clinical photoacoustic imaging: Current and future trends," *Photoacoustics,* vol. 16, p. 100144, Dec 2019, doi: 10.1016/j.pacs.2019.100144.

[2] R. Manwar, M. Zafar, and Q. Xu, "Signal and Image Processing in Biomedical Photoacoustic Imaging: A Review," *Optics,* vol. 2, no. 1, pp. 1-24, 2020, doi: 10.3390/opt2010001.

[3] D. Das, A. Sharma, P. Rajendran, and M. Pramanik, "Another decade of photoacoustic imaging," *Phys Med Biol,* Dec 23 2020, doi: 10.1088/1361-6560/abd669.

[4] M. W. Schellenberg and H. K. Hunt, "Hand-held optoacoustic imaging: A review," *Photoacoustics,* vol. 11, pp. 14-27, Sep 2018, doi: 10.1016/j.pacs.2018.07.001.

[5] S. Hakakzadeh and Z. Kavehvash, "Blind Angle and Angular Range Detection in Planar and Limited-View Geometries for Photoacoustic Tomography," in *2021 29th Iranian Conference on Electrical Engineering (ICEE)*, 2021 2021: IEEE.

[6] M. Xu and L. V. Wang, "Universal back-projection algorithm for photoacoustic computed tomography," *Physical Review E,* vol. 71, no. 1, 2005, doi: 10.1103/physreve.71.016706.

[7] S. K. Kalva and M. Pramanik, "Experimental validation of tangential resolution improvement in photoacoustic tomography using modified delay-and-sum reconstruction algorithm," *Journal of Biomedical Optics,* vol. 21, no. 8, p. 086011, 2016. doi: 10.1117/1.JBO.21.8.086011.

[8] J. Xiao, X. Luo, K. Peng, and B. Wang, "Improved back-projection method for circular-scanning-based photoacoustic tomography with improved tangential resolution," *Appl Opt,* vol. 56, no. 32, pp. 8983-8990, Nov 10 2017, doi: 10.1364/AO.56.008983.

[9] B. Wang, T. Ye, G. Wang, L. Guo, and J. Xiao, "Approximate back - projection method for improving lateral resolution in circular - scanning - based photoacoustic tomography," *Medical Physics,* 2021.

[10] S. Hakakzadeh and Z. Kavehvash, "Image Quality Equations for Focused Transducer in Circular Photoacoustic Computed Tomography " in *2021 29th Iranian Conference on Electrical Engineering (ICEE)*, 2021: IEEE.

[11] L. Nie, Z. Guo, and L. V. Wang, "Photoacoustic tomography of monkey brain using virtual point ultrasonic transducers," *J Biomed Opt,* vol. 16, no. 7, p. 076005, Jul 2011, doi: 10.1117/1.3595842.

[12] M. Kim, G. S. Jeng, I. Pelivanov, and M. O'Donnell, "Deep-Learning Image Reconstruction for Real-Time Photoacoustic System," *IEEE Trans Med Imaging,* vol. 39, no. 11, pp. 3379-3390, Nov 2020, doi: 10.1109/TMI.2020.2993835.

[13] B. Treeby and B. Cox, "k-Wave: MATLAB toolbox for the simulation and reconstruction of photoacoustic wave fields," *Journal of Biomedical Optics,* vol. 15, no. 2, p. 021314, 2010.